TITLE: Uneven missing data skews phylogenomic relationships within the lories and lorikeets

Brian Tilston Smith[1]*, William M. Mauck III[1,2], Brett Benz[3], and Michael J. Andersen[4]

[1]*Department of Ornithology, American Museum of Natural History, Central Park West at 79th Street, New York, NY 10024, USA*

[2]*New York Genome Center, New York, NY 10013, USA*

[3]*Museum of Zoology and Department of Ecology and Evolutionary Biology, University of Michigan, Ann Arbor, MI 48109, USA*

[4]*Department of Biology and Museum of Southwestern Biology, University of New Mexico, Albuquerque, New Mexico, 87131, USA*

*Corresponding Author: Brian Tilston Smith, *Department of Ornithology, American Museum of Natural History, Central Park West at 79th Street, New York, NY 10024, USA; Email address: briantilstonsmith@gmail.com*

Keywords.—bird, phylogeny, parrot, likelihood, museum specimen, museum DNA

Abstract

Resolution of the Tree of Life has accelerated with advances in DNA sequencing technology. To achieve dense sampling, it is often necessary to obtain DNA from historical museum specimens to supplement modern genetic samples. However, DNA from historical material is generally degraded and fragmented, which presents various challenges. In this study, we evaluated how the read depth at variant sites and missing data among historical and modern sample types impacts phylogenomic inference. We explored these patterns in the brush-tongued parrots (lories and lorikeets) of Australasia by sampling ultraconserved elements in 105 taxa. Trees estimated with low coverage sites had several clades where historical or modern samples clustered together, which were not observed in trees with more stringent filtering. To assess if the aberrant relationships were affected by missing data, we performed an outlier analysis of sites and genes for trees built with and without low coverage sites, and with and without missing data. Outlier analyses showed that 6.6% of total sites were driving the topological differences, and at these sites, historical samples had 7.5x more missing data. An examination of subclades found loci biased by missing data, and the exclusion of these loci shifted phylogenetic relationships. Predictive modeling found that outlier analysis scores were not correlated with summary statistics of locus alignments, indicating that outlier loci do not have characteristics differing from other loci. After accounting for biased loci and understanding the stability of relationships, we inferred a more robust phylogenetic hypothesis for lories and lorikeets.

Introduction

Historical and ancient DNA from museum specimens is widely employed for incorporating rare and extinct taxa in phylogenetic studies (e.g., Thomas et al. 1989; Mitchell et al. 2014; Fortes et al. 2016). The inclusion of these samples has helped discover and delimit species (Helgen et al. 2013; Paijmans et al. 2017), resolve phylogenetic relationships (Mitchell et al. 2016), and clarify biogeographic history (Kehlmaier et al. 2017; Yao et al. 2017). DNA sequences obtained from dry and alcohol-preserved museum specimens have been collected using a range of techniques, including Sanger sequencing (Sorensen et al. 1999), restriction site-associated DNA sequencing (Tin et al. 2015; Ewart et al. 2019), and sequence capture of reduced (McCormack et al. 2016; Ruane et al. 2017; Linck et al. 2017) or whole genomes (Hung et al. 2014; Enk et al. 2014). However, DNA sequences collected from these museum specimens are subject to errors associated with contamination (Malmström et al. 2005), DNA degradation (Briggs et al. 2007; Sawyer et al. 2012), and low coverage in read depth (Tin et al. 2015), which all present challenges in distinguishing evolutionary signal from noise.

Sequence capture of ultraconserved elements (UCEs) is a popular approach for collecting orthologous genomic markers in phylogenomic studies (Faircloth et al. 2015; Chakrabarty et al. 2017; Esselstyn et al. 2017) and is increasingly used for historical specimens (McCormack et al. 2016; Hosner et al. 2016; Ruane et al. 2017). A common finding is that the loci recovered are typically shorter in older samples (McCormack et al. 2016; Hosner et al. 2016; Ruane et al. 2017). Shorter loci are potentially problematic because the sequence capture approach targets the invariable UCE core, limiting the portion of the flanking region that contains polymorphic sites, so shorter loci potentially contain less information. Another factor that may cause differences among historical and modern samples is that phylogenomic pipelines that do not involve variant calling, typically employ read-specific filtering, where the average read depth across all sites in a locus is used to determine whether the locus is excluded. Under this type of scenario, low coverage sites may not be identified by typical filters, exacerbating differences among historical and modern samples. Although some studies only use DNA sequences collected from historical or ancient samples (e.g., Hung et al. 2014), most phylogenetic approaches involving non-contemporaneous samples combine data. For those that do use DNA from both sample types, additional challenges in downstream analyses may arise due to an asymmetry in the phylogenetic signal caused by missing data (e.g., Hosner et al. 2016).

The impact of missing data on phylogenetic inference remains contentious (Lemmon et al. 2009; Simmons 2012; Wiens and Morrill 2011; Hovmöller et al. 2013; Simmons 2014; Jiang et al. 2014; Streicher et al. 2015). Findings suggest that even when a large proportion of sites have no data,

phylogenetic signal is retained if enough characters are present (Philippe et al. 2004; Roure et al. 2012; Shavit Grievink et al. 2013; Molloy and Warnow 2017). In contrast, missing data have also been shown to bias phylogenetic relationships, particularly when the missing sites are non-randomly distributed (e. g., Lemmon et al. 2009; Simmons 2012; Simmons 2014). Bias may manifest as inflated support values and erroneous branch lengths, or as inconsistency between optimality criteria or phylogenomic approaches (i.e., concatenation vs the multi-species coalescent). The increased availability of phylogenomic data has provided a more nuanced look at missing data's effect on phylogenetic inference (Philippe et al. 2004; Huang and Knowles 2014; Streicher et al. 2015; Xi et al. 2015). One means of dealing with missing data in phylogenomic datasets is to filter loci based on the proportion of either missing sites or missing species in the dataset (Hosner et al. 2016). However, this approach may not directly target problematic regions of an alignment, and phylogenetically informative signal may be discarded unnecessarily. A more direct approach would entail identifying which specific sites or genes are influenced by missing data.

Analyses of outlier sites or loci in phylogenomic data indicate that a small portion of genes can have a large impact on a topology (Shen et al. 2017; Arcila et al. 2017; Brown and Thomson 2017; Walker et al. 2018). These conflicting genealogies can be due to biological processes (e.g., incomplete lineage sorting; introgression; horizontal gene transfer) or to spurious phylogenetic signal caused by poor alignments, paralogy, and/or sequencing error. Putative outlier loci have been identified using topology tests (Arcila et al. 2017; Esselstyn et al. 2017), Bayes factors (Brown and Thomson 2017), and site/gene-wise log-likelihood differences among alternative topologies (Shen et al. 2017; Walker et al. 2018). Support for particular phylogenetic hypotheses may be driven by a small subset of loci (Brown and Thomson 2017; Walker et al. 2018), and the targeted removal of outlier loci can reconcile differences among topologies. Outlier analyses provide a framework for assessing how differences between historical and modern DNA sequences impact phylogenetic inference. In this study, we performed site and gene likelihood outlier analyses to evaluate whether sequence coverage and missing data impacts phylogenetic relationships in our focal group, the Loriini.

Lories and lorikeets, commonly known as the brush-tongued parrots, are a speciose clade (Tribe: Loriini) of colorful birds that are widely distributed across the Australasian region (Forshaw et al. 1989). The characterization of distributional ranges, phenotypic variation, and systematics of the clade was the product of expansive biological inventories that peaked during the early 1900s (Mivart 1896; Forshaw et al. 1989). The geographical extent of this work encompasses thousands of large and small islands spread across many countries in the Australasian region. Given these immense logistical constraints, modern collecting expeditions that aim to produce voucher specimens with genetic samples for continued systematic work (e.g., Kratter et al. 2006; Andersen et al. 2017) have been much more focused in scope

relative to the pioneering work of the 20th century that produced extensive series of specimens across species' entire ranges (e.g., Mayr 1933; Mayr 1938; Mayr 1942; Amadon 1943). Thus, the lack of modern genetic samples means that phylogenetic relationships in many groups, like the Loriini, remain unresolved. To get around this constraint, phylogenomic studies have sourced DNA from historical specimens to fill modern sampling gaps (Moyle et al. 2016; Andersen et al. 2018).

Prior phylogenetic work on the Loriini showed evidence for at least three paraphyletic genera (*Trichoglossus*, *Psitteuteles*, and *Charmosyna*) and highlighted the need for increased taxon and genomic sampling to more fully resolve relationships among taxa (Schweizer et al. 2015). To this end, we collected UCEs from 105 described taxa in the Loriini. Our sampling design used DNA isolated from fresh tissues (hereafter modern) and historical specimens, including some over 100 years old (hereafter historical; supplementary fig. S1; supplementary table S1). We anticipated challenges with processing, recovering, and analyzing UCEs from historical specimens, and expected that biases in the DNA sequence data might yield misleading phylogenetic signal. To evaluate biased phylogenetic signal and explore options for maximizing the amount of data recovered, we produced alignments using different coverage thresholds and performed a series of tests that evaluated the information content and topological stability. Specifically, we used site-wise and gene-wise likelihoods to identify which portions of the alignment drive topological differences among trees 1) estimated with and without low coverage sites, and 2) with and without missing data. We produced a series of trees with differing subsets of putative outliers removed and quantified the change in topology using a tree distance metric and support values, and summarized the information content of each locus. Next, we assessed whether the likelihood scores from the outlier analyses could be predicted by locus-specific alignment statistics. After rigorously assessing potential biases in the data we propose a phylogenetic hypothesis for lories and lorikeets.

Results

Data characteristics

We sequenced 176 unique samples, including 16 that were re-sequenced to improve the amount of data recovered. We dropped five individuals that had aberrant relationships and long branches in the tree, patterns that were presumably driven by limited data. The final dataset comprised 171 unique individuals (168 ingroup, three outgroup). We produced two separate datasets that included all variant sites irrespective of coverage (hereafter Low Coverage dataset), and a second set that excluded variant sites with less than 6x coverage using bcftools (hereafter Filtered dataset). In the Low Coverage and Filtered datasets, loci had a mean length of 498 bps (range: 136–1,708 bps) and 482 bps (range: 105–1,413 bps), respectively. The mean and range number of taxa per locus was 164 for the Low

4

Coverage (48–171) and 152 for the Filtered (5–171) datasets. After retaining loci where 75% of the individuals were present in any one locus, the Low Coverage dataset had 4,212 loci, 2,112,365 bps and 58,762 parsimony informative sites, whereas the Filtered concatenated alignment had 3,775 loci, 2,046,673 bps and 51,482 parsimony informative sites. We classified samples into two categories: 1) samples that were collected within the last 30 years and came from frozen or ethanol preserved tissue (hereafter Modern), and 2) samples that came from dry museum skins with ages ranging from the 1960s through the late 1800s (hereafter Historical).
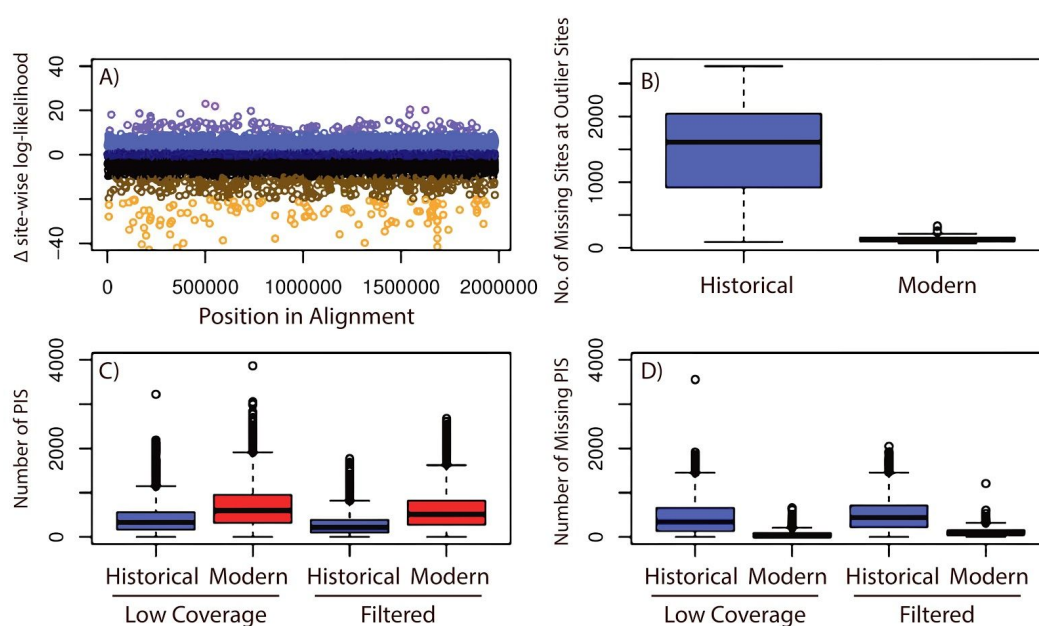
Outlier sites and loci

FIG. 1. Historical samples have less information than modern samples, particularly at outlier sites. A) Outlier site plot showing Δ sites-wise log-likelihoods (Δ s-lk) for topologies estimated with and without low coverage sites. The y-axis is the Δ s-lk score and the x-axis represents individual loci in the concatenated alignment. Points are colored according to the magnitude of the Δ site-wise log-likelihood scores according to a gradient ranging from > 20 (red) through less than -10 (yellow). B) Boxplot of historical (blue) and modern (red) samples showing the amount of missing data in the 3,142 outlier sites (Δ s-lk < -2) identified in plot A. C) and D) Boxplot showing the number of parsimony informative sites (PIS) and number of missing sites at parsimony informative sites, respectively.

We performed outlier analyses assessing the change in site-likelihoods scores (hereafter Δ s-lk) for the Low Coverage (T_1) versus the Filtered topology(T_2)—Δ s-lk = T_1 site log-likelihood - T_2 site

log-likelihood. The analyses identified 3,142 (3,142 sites: Δ s-lk < -2; 489 sites: Δ s-lk < -10 = 489; 118 sites: Δ s-lk < -20) and 1,933 (1,933 sites: Δ s-lk > 2; 113 sites: Δ s-lk > 10; 4 sites Δ s-lk > 20) outlier sites in the alignment (2,112,365 bps) with negative and positive Δ s-lk values, respectively (fig. 1A). Higher and more positive Δ s-lk are sites that better support the topology estimated from the Filtered alignment, and lower and more negative values favor the tree estimated from the Low Coverage alignment. The 3,142 outlier sites with negative Δ s-lk were found on 1,904 loci, and the 1,933 outlier sites with positive values were on 1,378 loci. The 3,142 sites with Δ s-lk < -2, which favored the topology of the Low Coverage tree, exhibited a disproportionate number of missing sites in the historical versus modern samples (fig. 1B). We do not discuss the number of missing sites for sites Δ s-lk > 2 because positive sites favor relationships in the Filtered tree.

We performed a complementary outlier analysis assessing six subclades within the Lorrini. For this outlier analyses we inferred topologies for each subclade using alignments without (T_1) and with missing data (T_2)—Δ g-lk = T_1 gene log-likelihood - T_2 gene log-likelihood. More negative Δ g-lk would indicate the topology estimated with missing data removed was preferred, and more positive values support the topology estimated with missing data included. Overall, outlier analyses on the Low Coverage alignment identified more outlier loci (fig. 2 and supplementary fig. S2). There were 47/4 (Low Coverage/Filtered), 371/35, and 1,730/518 loci in the three bins (Δ g-lk of: > 20, > 10, and > 2), respectively (fig. 2). There were 122/11 (Low Coverage/Filtered) and 1,336/316 loci in the three bins (Δ g-lk of: < -10 and < -2), respectively. The maximum and minimum Δ gene-wise log-likelihood were much higher in the Low Coverage (in *Trichoglossus*/*Eos*/*Psitteuteles*/*Glossopsitta*: Δ g-lk = -31.926–476.093) versus the Filtered dataset (in *Trichoglossus*/*Eos*/*Psitteuteles*/*Glossopsitta*: Δ g-lk = -18.247–41.402). There were 1,305 loci identified by both outlier analyses—the Low Coverage versus Filtered tree and subclade. In the Low Coverage and Filtered analysis, the outlier sites were found on 599 loci uniquely identified, and 425 loci identified by the subclade clade analyses.
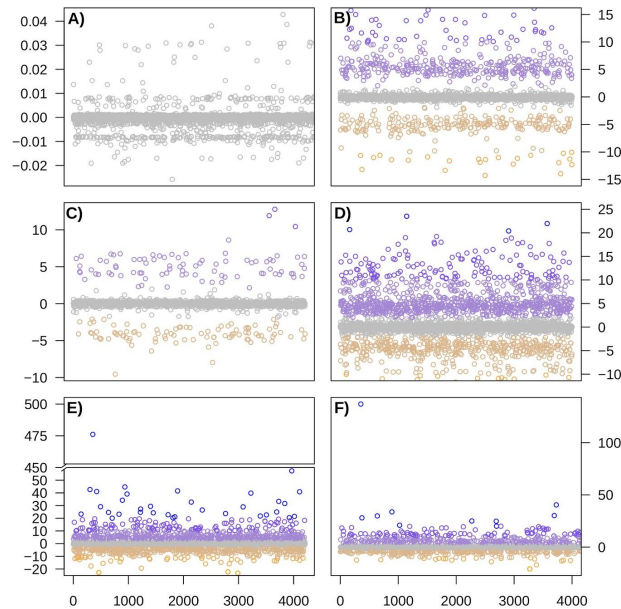
6

FIG. 2. Likelihood plots showing Δ gene-wise log-likelihoods (Δ g-lk) for topologies estimated with and without missing data for the Low Coverage dataset. The y-axis is the Δ gene-wise log-likelihood and the x-axis represents individual loci across the full alignment. Shown are the results for six subclades assessed within Loriini using the Low Coverage dataset: a) *Eos*, *Trichoglossus*, *Glossopsitta concinna*, and *Psitteuteles iris*, b) *Parvipsitta* and *Psitteuteles*, c) *Neospittacus*, d) *Chalcopsitta* and *Pseudeos*, e) *Lorius*, and f) *Charmosyna*, *Vini*, and *Phigys*. Points are colored according to the magnitude of the Δ g-lk scores according to a gradient ranging from of > 20 (blue) through < -10 (orange).

We built a neural net to test whether the Δ gene-wise log-likelihood of each gene partition could be predicted by the alignment statistics. Alignment statistics were weak predictors of Δ gene-wise log-likelihood scores in the Low Coverage versus Filerted trees (mean and SD R^2 =0.05 (0.03); RMSE=0.03 (0.01) Δ gene-wise log-likelihood scores. In the model GC content (Mean Variable Importance: GC content=31.54) and number of parsimony informative sites (25.14) were more important than the others (Alignment Length=12.89; No. of Taxa=12.89; Undetermined Characters=12.41; No. Variable sites=1.32). The subclade neural nets generally performed more poorly with R^2 values ranging from 0.002–0.08, and parsimony informative sites and number of variable sites were the most important variables (Supplementary Table S2). These results suggest that the loci with higher Δ g-lk values had higher parsimony informative sites, but there was no general trend between these variables across all loci.

7

Resolving phylogenomic relationships among lorikeets

The backbone phylogeny we inferred for the Loriini generally had high support and the placement of genera was stable (supplementary figs. S3–S14). Summarizing higher-level relationships, *Oreopsittacus* was sister to all other ingroup taxa, then *Charmosyna* was sister to the clade containing *Neopsittacus*, *Lorius*, *Pseudeos*, *Chalcopsitta*, *Psitteuteles*, *Glossopsitta*, *Eos*, *Trichoglossus*, and *Parvipsitta*. The placements of *Neopsittacus*, *Lorius*, *Pseudeos*, and *Chalcopsitta* were well-supported in the tree, and each of these genera were monophyletic. *Trichoglossus*, *Charmosyna*, and *Psitteuteles* were not monophyletic. *Psitteuteles* was found in three separate places in the tree: *P. versicolor* was sister to the recently erected genus *Parvipsitta*; *P. iris* was nested within a clade of *Trichoglossus* taxa that are from Indonesia; and *P. goldei* was sister to the clade containing *Glossopsitta*, *Eos*, *Trichoglossus,* and *P. iris*. *Vini* and *Phigys* are strongly supported as nested within *Charmosyna*. Relationships within *Charmosyna* (including *Vini* and *Phigys*) and *Chalcopsitta* were generally stable across filtering schemes, as were relationships of the less diverse clades (*Oreopsittacus*, *Neopsittacus*, and *Parvipsitta*). Within the remaining clades, there were several notable differences in topological relationships among the Low coverage and Filtered trees.
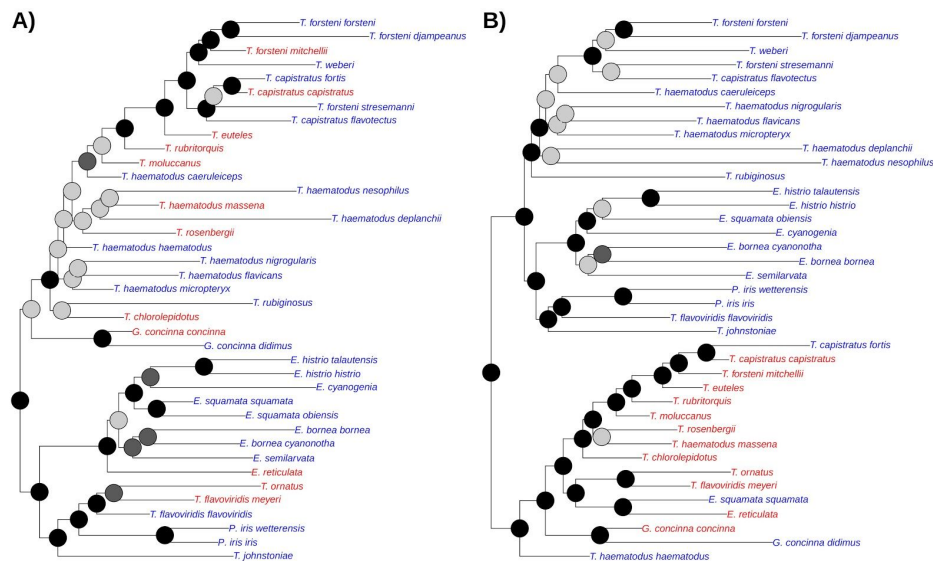

FIG. 3. In the Low Coverage tree are clades composed of mostly historical versus modern samples. Shown is the subclade containing *Trichoglossus*/*Eos*/*Psitteuteles iris*/*Glossopsitta* from trees estimated without (A: Filtered Tree) and with low coverage sites (B: Low Coverage Tree). Bootstrap nodes are

colored on a gradient from 100% (black) to < 70% (gray). Taxon names are colored according to whether their DNA came from modern tissues (red) or historical specimens (blue).

The Filtered tree contains four clades containing *Trichoglossus*, *Eos*, *P. iris*, and *G. concinna* with varying levels of support (fig. 3B). *Glossopsitta concinna* was sister to a clade containing a monophyletic *Eos*, *Trichoglossus*, and *P. iris*. Within this tree, *Eos* was monophyletic and sister (BS = 100%) to a clade containing *Trichoglossus* taxa that occur in Indonesia and the Philippines (*T. ornatus*, *T. flavoviridis*, and *T. johnstoniae*) and *P. iris*. The *Eos*, *Trichoglossus*, and *P. iris* clade was sister (BS = 85%) to a clade containing the remaining *Trichoglossus,* which was supported by a bootstrap value of 91%. This *Trichoglossus* clade had several short internodes and poorly supported relationships, particularly among *T. haematodus* subspecies, which primarily came from historical samples. *Trichoglossus euteles*, *T. forsteni*, *T. capistratus*, *T. weberi*, and *T. rubritorquis* are nested within *T. haematodus*. *Trichoglossus forsteni stresemanni* was more closely related to *T. capistratus* then to other *Trichoglossus forsteni* taxa. In contrast, the Low Coverage tree has two well-supported (BS > 95%) clades comprised of *Trichoglossus*, *Eos*, *P. iris*, and *Glossopsitta concinna* (fig. 3A). One clade consists of entirely historical samples ($N = 23$), whereas the other was primarily modern samples (13/16). Within each of these clades, tips have similar relationships among taxa as seen in the Filtered tree. *Trichoglossus* that occur in Indonesia or the Philippines and *P. iris* are sister to *Eos* and the remaining *Trichoglossus* form a clade with the exception of one historical sample (*T. haematodus haematodus*). Support values are higher in the clade composed of mostly modern samples. In both trees (Low Coverage and Filtered), *Charmosyna* was composed of four clades, *C. wilhelminae* was sister to all other taxa in the clade, *C. rubronotata* and *C. placentis* are sister and form a clade, *C. multistriata* was sister to *C. josefinae* and *C. papou*, and the remaining *Charmosyna* taxa (*C. margarethae*, *C. rubrigularis*, *C. meeki*, *C. palmarum*, and *C. amabilis*) and *P. solitarius* and *Vini* form a clade. The position of *C. pulchella* and *C. toxopei* will be discussed below.

Similar clustering patterns based on sample type (historical versus modern) are observed in *Lorius*, *Vini*, and *Charmosyna* in the Low Coverage trees (supplementary fig. S3). The two subspecies of *L. lory* that come from modern samples are sister. The one modern sample of *C. placentis* was sister to *C. rubronotata*. *Charmosyna palmarum* (a modern sample) was strongly supported as sister to *Phigys* and *Vini*. The three *Vini* from historical samples group together. The two *C. papou* subspecies that come from historical samples are sister to a clade containing the remaining *C. papou* subspecies. None of these relationships are observed in the Filtered tree.

Impacts of filtering sites and loci

The removal of outlier loci with positive Δ g-lk scores broke-up some of the same-type clusters, particularly at a threshold value of all loci with Δ > 2 (supplementary figs. S4–S6). However, the removal of this many loci (n = 1,730) also reduced the support for other nodes in the tree. Trees estimated with the removal of negative outlier loci retained the apparent sample-type clusters (supplementary figs. S3, S7, S8). Individual taxa whose position varied the most among filtering schemes were *G. concinna* and *T. rubiginosus*, an aberrantly colored and geographically isolated taxon. In the Filtered dataset, which did not exhibit the sample-type clusters, the removal of outlier loci (Δ g-lk > 2; supplementary fig. S12) increased the support for the placement of *G. concinna* as sister to the clade containing *Trichoglossus*, *Eos*, and *P iris*. In contrast, the removal of outlier loci (Δ g-lk < -2) placed *G. concinna* within the clade containing *Trichoglossus*, *Eos*, and *P iris*. This placement received moderate bootstrap support for either being sister to the clade containing *T. haematodus* and allies or the entire clade containing *Trichoglossus*, *Eos*, *P. iris*, and *G. concinna*. *Lorius lory* has seven subspecies, which formed a well-supported clade in the Filtered tree (supplementary fig. S9), with the exception of *L. lory viridicrissalis*, whose placement was equivocal. The Low Coverage tree has *L. lory viridicrissalis* within the *L. lory* clade with low support (supplementary fig. S3). Filtering of outlier loci changed support values, but never unequivocally placed *L. lory viridicrissalis* within *L. lory*. *Charmosyna pulchella* and *C. toxopei* are sister taxa, however, their position within *Charmosyna* varied across trees. Trees estimated with all loci or loci with negative Δ g-lk scores excluded had these taxa as sister (often with high support) to the clade containing the subclades *C. multistriata*; *C. josefinae* and *C. papou*; and *C. margarethae*, *C. rubrigularis*, *C. meeki*, *C. palmarum*, *C. amabilis*, *P. solitarius*, and *Vini* (supplementary figs. S7 and S8). Alternatively, trees where positive Δ g-lk scores were excluded had these taxa as sister, albeit with lower support (BS = 72% and 79%) to a clade containing *Charmosyna*, *Phigys*, and *Vini* (supplementary figs. S4–S6).

Examining the differences among topologies in multi-dimensional space showed distances among trees change across filtering schemes (fig. 4). In the trees where outlier sites were excluded (fig. 4A), the Robinson-Foulds distances among the Low Coverage and Filtered trees decreases. At a filtering threshold of Δ s-lk < -2 (3,142 sites), the distance between the two trees was minimal. Filtering sites with positive Δ s-lk values maintained a topology similar to the Low Coverage tree, except at a threshold of Δ s-lk > 2, which was distant from all other trees in multi-dimensional space. In the subclade analyses, the filtering of loci did not yield similar topologies between the Low Coverage and Filtered trees (fig. 4B). However, the Low Coverage tree where loci were excluded at a threshold of Δ s-lk > 2 was the least distant from the Filtered tree. The Low Coverage trees with all loci and Δ s-lk < -2 produced similar topologies and were

10

the most distant from the Filtered trees. Despite some differences in the placement of taxa across the Filtered trees, the Robinson-Foulds distances among trees were comparatively low.
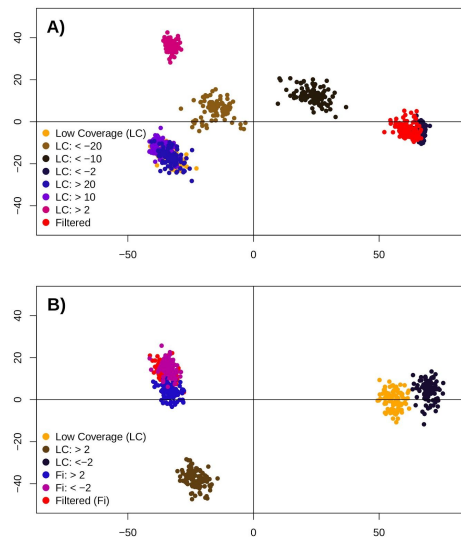

FIG. 4. Multidimensional scaling of Robinson-Foulds distances among 100 bootstrap trees with differing levels of outlier sites or loci excluded. Plot A compares distances among Filtered and Low Coverage trees where outlier sites have been removed at different increments. Outlier sites were excluded in the Low Coverage alignment using Δ site-wise log-likelihood (Δ s-lk) thresholds of: >20, >10, >2, <-2, <-10, and <-20. Plot B shows the distances among trees produced from the subclade outlier analyses. Shown is a comparison of the Low Coverage and Filtered trees with topologies estimated with outlier loci excluded using Δ gene-wise log-likelihood (Δ g-lk) thresholds of: >2 and <-2.

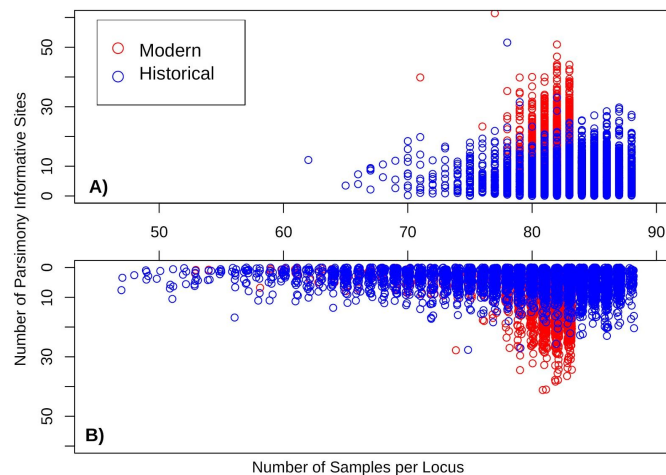**Modern versus historical samples**

11

FIG. 5. Mirror plot showing how the number of samples and parsimony informative sites change between the Low Coverage (A) and Filtered (B) alignments. Each dot represents a locus that was colored according to whether the sample was from modern tissues (red) or historical specimens (blue). On the x-axis is the number of taxa in each locus alignment, and on the y-axis is the number of parsimony informative sites in each locus alignment.

Overall, the Low Coverage dataset had 1.4x more parsimony informative sites than the Filtered dataset (fig. 1C). For each alignment type, the modern samples contained a greater number of parsimony informative sites and less missing data than the historical samples (1.7x and 2.2x more parsimony informative sites in the Low Coverage and Filtered datasets, respectively; fig. 1D). A comparison of sample types shows the range in number of parsimony informative sites among loci was lower in the modern samples in contrast to the historical samples (fig. 5). In the Filtered dataset, the number of parsimony informative sites dropped, and the range of the number of individuals in each locus alignment increased. The percentage of missing data in samples decreased with specimen age (Adjusted R^2 = 0.51; n = 144; p-value < 0.0001; supplementary fig. S15). A qualitative assessment of batch effects, by coloring each tip in the tree according to sequencing run, did not detect biases whereby samples would have clustered together based on sequencing plate (supplementary figs. S16 and S17). In the Low Coverage tree (supplementary fig. S18), biases in clustering was more apparent when tips are colored according to whether the sample came from modern or historical source, which was not observed in the Filtered tree (supplementary fig. S19).

Discussion

We showed that systematic bias caused by missing informative sites between DNA sequence from modern versus historical specimens can produce aberrant or unstable phylogenetic relationships. To obtain dense taxon sampling in our focal group, the Loriini, we leveraged samples collected over the last 100 plus years and assessed how this sampling scheme impacted phylogenetic relationships by producing alignments with low coverage sites included and excluded. These two trees exhibited some striking differences. In the Low Coverage tree, there were numerous cases where historical or modern samples clustered together that were not observed in the Filtered tree. A site outlier analysis showed that a small number of sites (6.6% of total sites) were driving the topological differences, and at these sites, historical samples had 7.5x more missing data. Excluding low coverage sites reduced the discrepancy in missing data to a 4.5x difference between historical and modern samples, and at this level of disparity, the tree did not contain sample-type clusters. A more nuanced look at outlier loci within subclades showed that many loci supported alternative topologies when sites with missing data were excluded, and the position of

12

some branches shifted when these loci were excluded. Summary statistics of locus alignments were poor predictors of the likelihood scores used to identify outlier portions of the alignment, indicating that biased loci do not have characteristics differing from other loci. After accounting for biased loci and understanding the stability of nodes, we inferred a more robust phylogenetic hypothesis for the Loriini. Taxonomic relationships within the clade can now be revised to reflect natural groupings, but for some groups, additional work is still necessary.

Asymmetric information content among sample types

By including low coverage sites we were able to explore potential biases that can arise between historical and modern samples. Filtering according to a read coverage threshold at each variant site is common practice in population genomic studies (e.g., Thom et al. 2018), but this approach is less frequently employed in phylogenomic bioinformatic pipelines (e.g., Faircloth 2015). In the Low Coverage tree, we found clusters of historical or modern samples that were not present in the Filtered tree. These clusters could be caused by sequencing errors present in one sample type, batch effects, or by an asymmetry in informative sites. We had limited power to test for batch effects because we did not randomly and evenly sequence samples across runs, therefore there are portions of the tree where clades are composed almost entirely of samples from the same sequencing run. In these cases, we do not interpret these patterns as batch effects because the tips occur in their expected topological position and samples from different sequencing lanes are distributed throughout the tree. We also estimated multi-coalescent species trees and found similar patterns to those observed in the concatenated results, suggesting the biases in phylogenetic inference causing historical and modern samples to fall into separate clades may also impact approaches that take into account gene tree heterogeneity. However, we did not present those analyses because the species trees had overall low support, presumably because of low phylogenetic informativeness of individual gene trees. Our analyses suggest an asymmetry in phylogenetic information content among sample types is the primary culprit because of the 3,142 sites that drove the topological differences among trees, the historical samples had 7.5x more missing data at these sites. Although we cannot rule out sequencing error biasing some aspect of our phylogenetic inference, the topology within each of the most apparent sample-type clusters in the *Trichoglossus*/*Eos*/*Psitteuteles* clade exhibited the expected relationships among taxa.

Our complimentary outlier analysis on subclades also found loci that were impacted by missing data. In the Low Coverage tree, the sample-type clusters were broken up when outlier loci with positive values were excluded but also reduced support values. The exclusion of outlier loci with negative values retained the biased relationships. These loci had negative values because the topologies estimated with all

13

sites with missing data removed were more likely given the alignment. The removal of these loci produced alignments that only included loci that were either biased or not impacted by missing data. In the Filtered dataset, the number of identified outlier genes was reduced and exclusion of outlier loci was less profound. Nonetheless, the removal of outlier loci in the Filtered dataset showed how the placement of *G. conccina*, *T. rubiginosus*, and the clade containing *C. pulchella* and *C. toxopei* was sensitive to missing data. Interesting, about 75% of the loci identified by the subclade outlier analyses were the same loci of the outlier sites identified by the Low Coverage versus Filtered outlier analysis. The information content of the non-overlapping loci is important because the more targeted site-wise outlier analysis was better at reconciling topological differences among the Low Coverage and Filtered trees than was the subclade approach.

Identifying biased samples and loci

Our neural net models were not able to predict Δ gene-wise log-likelihood scores, but the number of parsimony informative sites was often the most important variable in the models. An explanation for the low predictability of the models was that even though the loci with high Δ g-lk scores tended to have a higher number of parsimony informative sites, there were also a large number of loci with high information content with low scores. The collective findings of the neural net models suggest that systematic bias associated with the characteristics of a locus alignment such as GC content or sequence length did not explain why loci were detected in the outlier analyses. Instead, the inability of the model to predict outlier scores indicates that biases in the loci were randomly distributed across phylogenetic informative loci.

Preferentially selecting phylogenetically informative loci is expected to produce trees with better support (Gilbert et al. 2018), but our results suggest that this practice can produce less reliable relationships when the data content dramatically varies among samples. Other work has shown that filtering phylogenomic markers by information content had mixed results in terms of resolving discordance among trees estimated with different phylogenetic methods (Mclean et al. 2018). As indicated by our neural net models, predicting which loci are biased by missing informative sites in some samples is not predictable based on characteristics of the locus. Outlier analysis using site and gene likelihood scores (Shen et al. 2017; Walker et al. 2018) provide a rapid means of identifying loci that have a large impact on a phylogeny reconstruction, but as we showed the resolution of this approach will depend on the trees that are available for comparison (e.g., expected relationship versus alternative phylogeny). Another, non-quantitative means of assessing the position of branches, which have high missing informative sites, is the tendency for samples to fall outside of their clade or even the ingroup, as

evident in previous phylogenomic studies on birds (Hosner et al. 2016; Moyle et al. 2016; Andersen et al 2019; McCullough et al. 2019). This was the case for seven of our excluded samples, which produced limited data and could not be accurately placed in their genus or higher-level clade. The sample-type clusters within *Trichoglossus/Eos/Psitteuteles* is an extreme example of this pattern, and the pattern is so striking because of the high number of historical samples in this particular clade.
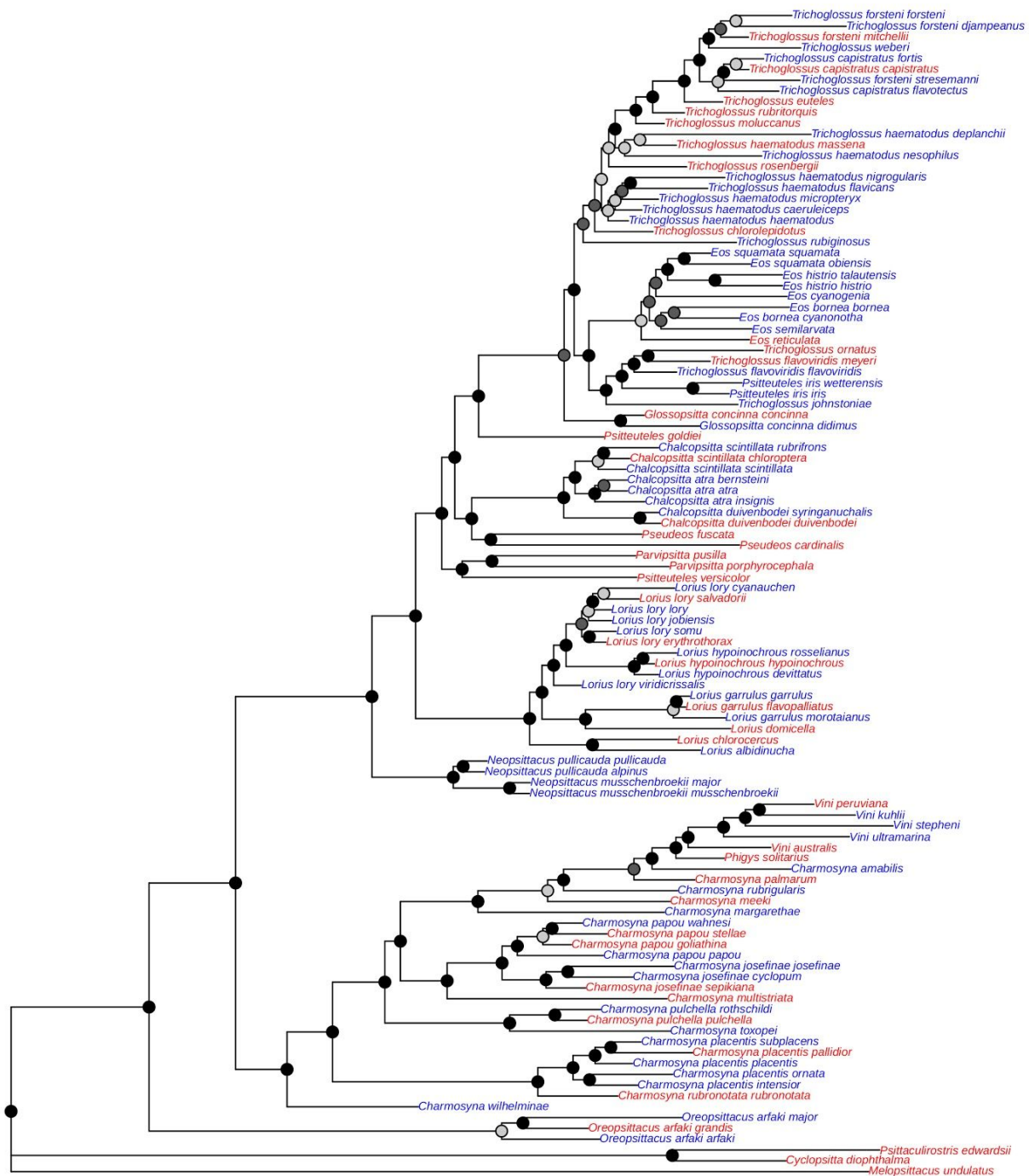
FIG. 6. Maximum likelihood tree containing unique taxa in Loriini. The tree was inferred from a concatenated alignment where loci identified with the gene likelihood analysis with Δ gene-wise log-likelihood (Δ g-lk) values of > 10 were excluded. On each node are shown rapid bootstrap values and the taxon names are colored according to their DNA came from modern tissues (red) or historical specimens (blue). Bootstrap nodes are colored on a gradient from 100% (black) to < 70% (gray).

Taxonomic implications

Our study builds on previous phylogenetic work on the Loriini by further clarifying relationships and adding 64 previously unsampled taxa (fig. 6). We inferred a backbone phylogeny of relationships among genera that was fairly well-resolved with the exception of the clade containing *Trichoglossus*, *Psitteuteles iris*, *Eos*, and *Glossopsitta* and some nodes in *Charmosyna*. Our analyses corroborated recently proposed taxonomic changes where *Pseudeos cardinalis* was moved into *Pseudeos* from *Chalcopsitta*, and *Parvipsitta* was resurrected to contain *P. pusilla* and *P. porphyrocephala*, which were previously placed in *Glossopsitta* (Schweizer et al. 2015). In all of our trees, *P. fuscata* and *P. cardinalis* were sisters and were in turn sister to *Chalcopsitta*. *Parvipsitta pusilla* and *P. porphyrocephala* were sisters and not closely related to *G. concinna*. However, we found strong support for *P. pusilla* and *P. porphyrocephala* being sister to *Psitteuteles versicolor*, a novel result. *Psitteuteles versicolor* and *Parvipsitta* could be subsumed under a single genus. Irrespective of this taxonomic decision, the polyphyly of *Psitteuteles* will require that *P. goldei* and *P. iris* be moved into new genera. *Psitteuteles goldei* is sister to the clade containing *Trichoglossus*, *Eos*, *P. iris*, and *Glossopsitta*. The taxonomic revision of *P. iris* will depend on how *Trichoglossus* is treated, as *P. iris* is nested within a geographically coherent clade of taxa distributed largely to the west of New Guinea. The clade containing *Charmosyna*, *Phigys*, and *Vini* represents a deep, diverse, and geographically widespread group. The species in these genera are varied in terms of body size and shape, tail length, plumage color, and sexual dimorphism (Forshaw et al. 1989; Merwin et al. 2019), and these morphological traits are not found in monophyletic groups in our phylogeny. Species-level relationships among species in *Charmosyna* were well-supported and stable with the exception of the placement of *C. toxopei* and *C. pulchella*. Overall, the taxonomic revision of this clade will present challenges regarding when and where to split or lump taxa and how best to circumscribe genera.

Relationships among subspecies within species varied substantially among taxa. Support for relationships among species within *Lorius* were generally stable except the placement of *L. lory viridicrissalis*, which was only nested within *L. lory* in the Low Coverage tree. Our *L. lory viridicrissalis*

16

was a historical sample with a high degree of missing parsimony informative sites and its position as sister to *L. lory* and *L. hypoinochrous* is most likely an artifact. There were also varying levels of support for relationships among the other subspecies in *L. lory,* the most diverse species in the genus. Relationships among subspecies in *C. papou*, *C. josefinae*, and *C. placentis* had high support. Our analyses inferred a paraphyletic *T. haematodus* (with low support) and *T. forsteni*, the latter of which is still included in *T. haematodus* by some taxonomic checklists (Clements et al. 2019; Dickinson and Remsen 2013). This clade had many historical samples, which likely contributed to the clade's low support, but even several of the taxa from modern samples were not placed with high support in the clade. Resolving these challenging relationships within *Trichoglossus* will likely require finer-resolution genetic data and expanded population-level sampling.

In conclusion

Next-generation sequencing has provided systematists with an unprecedented amount of information for inferring phylogenetic relationships (McCormack et al. 2013). However, phylogenomic datasets have come faster than the development of best practices for assembling, processing, and analyzing large datasets for phylogenetic inference, particularly from low-quality samples. Alignments produced without careful inspection may harbor biased loci that can have a large impact on downstream analyses (Springer and Gatesy 2018). Our findings have general implications for phylogenomic studies where there is an asymmetry in parsimony informative sites among closely related taxa. Although the impacts of missing data have shown ambiguous impacts on phylogenetic inference (Lemmon et al. 2009; Simmons 2012; Wiens and Morrill 2011; Hovmöller et al. 2013; Simmons 2014; Streicher et al. 2015), the combination of a much higher number of informative sites in contemporary phylogenomics with an asymmetry between samples of different quality warrants new investigations on biases that can arise in alignments. The magnitude of biases will likely vary according to clade diversity and age, and the number of loci collected. We found that the bias was most extreme in a diverse and rapid radiation where there was likely limited information, even in complete loci, for teasing apart relationships. Shallow systematic and phylogeographic studies are expected to be the most difficult temporal scale for resolving relationships when there are high missing data associated with particular samples. Moving forward, having an understanding of the informational content of a locus, and how that information affects genealogy, will help avoid inferring dubious phylogenomic relationships.

Materials and Methods

We sampled all 12 genera, 58/59 species, and 102 (Clements et al. 2019) of 112 named taxa

17

within the Loriini, and three additional subspecies (*Glossopsitta concinna concinna*, *G. concinna didimus*, and *Trichoglossus haematodus caeruleiceps*) recognized by Gill and Donsker (2019) and Forshaw (2010), respectively. In total, we sampled 105 taxa within Loriini. *Charmosyna diadema* is the only species not included in our study, which is extinct and known from a single female specimen (Forshaw et al. 1989). Two additional taxa (*Eos histrio talautensis* and *E. squamata riciniata*) produced few loci with high missing data in those loci and were excluded from final analyses. We did not obtain samples from the following taxa: *C. rubronotata kordoana*, *Psitteuteles iris rubripileum*, *Neopsittacus pullicauda socialis*, *E. histrio challengeri*, *T. haematodus brooki, and T. moluccanus septentrionalis*. We treated *T. haematodus rosenbergii as T. rosenbergii* and *T. haematodus intermedius* as *T. haematodus haematodus* following Gill

and Donsker (2019). We also followed Gill and Donsker (2019) and used *Parvipsitta* for *P. pusilla and P. porphyrocephala*. When possible, we sampled more than one individual per species to verify the phylogenetic position of a taxon. For outgroups, we used *Melopsittacus undulatus*, *Psittaculirostris edwardsii*, and *Cyclopsitta diophthalma*, which together with the Loriini form the clade Loriinae (Joseph et al. 2012; Provost et al. 2018). Sampling map and specimen details and locality information are available in supplementary fig. 1 and supplementary Table S1.

We extracted total genomic DNA from muscle tissue using QIAamp DNeasy extraction kits (Qiagen, Valencia, CA). For historical samples from museum specimens we used a modified DNeasy extraction protocol that used QIAquick PCR filter columns that size selected for smaller fragments of DNA. The modified protocol also included washing the sample with H_2O and EtOH prior to extracting as well as extra time for digestion. DNA extraction from historical samples was done in a dedicated lab for working with degraded samples to reduce contamination risk. We quantified DNA extracts using a Qubit 2.0 Fluorometer (Thermo Fisher Scientific). Library preparation of UCEs and enrichment, and Illumina sequencing were performed by RAPiD Genomics (Gainesville, FL). The Tetrapod UCE 5K probe set was used to enrich 5,060 UCE loci (Faircloth et al. 2012). The wetlab component of this study was carried out over three years and the number of individuals multiplexed per lane ranged from 48–384. Sequencing was done on an Illumina HiSeq 2500 PE 125 or HiSeq 3000 PE 150. Fastq files are available on the Sequence Read Archive (SRA Bioproject ID:498485).

We used a modified data-processing pipeline that incorporated PHYLUCE (Faircloth 2015), a software package developed for analyzing UCE data, and seqcap_pop (Smith et al. 2014; Harvey et al. 2016). We used fastq screen to map raw reads to bacterial genomes and filter contaminant DNA (Wingett and Andrews 2018). Low-quality bases and adaptor sequences were trimmed from multiplexed fastq files using illumiprocessor v1 (Faircloth 2013; Bolger et al. 2014). Next, reads were assembled into contigs

18

with Trinity v2.0.6 (Grabherr et al. 2011) and contigs were mapped to UCE probes. We chose the sample that produced the largest number of UCEs as the reference for subsequent mapping for all individuals. We generated an index of the reference sequence and independently mapped reads from each sample to the same reference sequence using BWA v0.7.13-r1126 (Li and Durbin 2009). SAM files produced from the BWA mapping were converted to BAM files, which were sorted with SAMtools (Li et al. 2009), and cleaned with Picard v1.106 (http://broadinstitute.github.io/picard). Then, we used the mpileup function in SAMtools to call variant sites and produce a VCF file, vcfutils to convert from VCF to fastq (excluding sites with quality scores < 20), and seqtk to convert fastq to fasta. From this last step, we produced two sets of DNA sequences that were analyzed independently. One dataset retained all variant sites irrespective of coverage (hereafter Low Coverage dataset), and a second set that excluded variant sites with less than 6x coverage using bcftools (hereafter Filtered dataset). These collective steps produced single fasta files containing all UCE loci for each individual sample. The following steps were independently performed for both datasets (Low Coverage and Filtered). Loci with greater than 30% missing sites were removed from each individual before alignment. In PHYLUCE we concatenated fasta files of each sample, aligned sequences in MAFFT (Katoh & Standley 2013), and retained loci where 75% of the samples were present in a locus for the final concatenated alignment.

Low Coverage and Filtered outlier analysis

We estimated trees with 171 tips, which included multiple individuals per taxon. This dataset was used to check if samples from the same taxon grouped together as a means of identifying problematic samples. To focus relationships among named taxa all subsequent analyses are based on a reduced dataset that contained one sample per taxon with 105 ingroup taxa and three outgroup samples. We estimated phylogenomic trees for both the Low Coverage and Filtered concatenated alignments containing only unique taxa in IQ-TREE (Nguyen et al. 2014) using ModelFinder (Kalyaanamoorthy et al. 2017) to select the best-fit substitution model for each gene partition (Chernomor et al. 2016). To assess support, we estimated 1000 rapid bootstraps. The trees from the two different alignments did not produce the same phylogenetic relationships, so we performed an outlier sites/gene analysis to identify which sites were causing the topologies to be different. We performed a two-topology, site-specific log-likelihood test that estimated the site-likelihoods based on the gene partition of the Low Coverage alignment using topologies estimated from the Low Coverage (T_1) and Filtered alignments (T_2) in RAxML (Stamatakis 2014). We then estimated the change in site-wise log-likelihoods (hereafter Δ s-lk = T_1 site log-likelihood - T_2 site log-likelihood). We binned putative outlier sites into bins representing Δ s-lk: >20, >10, >2, <-2, <-10, and <-20. We produced new concatenated alignments that corresponded to each Δ s-lk threshold bin, for

which outlier sites were converted to ambiguous sites (Ns) in all individuals. This approach allowed us to estimate trees with different levels of outlier sites removed from the alignment. Next, we converted the DNA sequence of each locus alignment into only parsimony informative sites using FASconCAT-G (Kück and Longo 2014), and summarized the amount of parsimony informative sites and missing data at these sites for modern and historical samples. To visualize how different the trees were, we measured the distance among 100 bootstrap trees using Robinson-Foulds distances (Robinson and Foulds 1981) with the multiRF function in phytools (Revell 2012) and used multidimensional scaling to plot the distances in two-dimensional space. All trees were processed and visualized using the R (R Core Team 2019) packages phytools and ape (Paradis et al. 2004). To visualize the distribution of each sample type on the tree we colored tips blue (historical) or red (modern).

Subclade outlier analyses

We performed a complementary outlier analysis assessing subclades, but in this set of analyses we compared trees estimated from alignments with and without missing data. By performing this analysis on subclades we were able to examine how missing data impacted different portions of the tree. This approach could not be applied to alignments containing all clades because at least one individual had missing data at every site in the alignment. The six clades including a single outgroup sample were based on preliminary phylogenetic analysis and were a) *Eos*, *Trichoglossus*, *Glossopsitta concinna*, and *Psitteuteles iris* ($n = 22$), b) *Parvipsitta* and *Psitteuteles* ($n = 8$), c) *Neospittacus* ($n = 7$), d) *Chalcopsitta* and *Pseudeos* ($n = 14$), e) *Lorius* ($n = 18$), and f) *Charmosyna*, *Vini*, and *Phigys* ($n = 32$). To produce a concatenated alignment for a clade, we followed the same steps listed above. To retain more sites in the larger clades we did not include redundant taxa or samples. We further reduced the sample size from 58 to 22 in the diverse clade containing *Eos*, *Trichoglossus*, *Psitteuteles iris*, and *Glossopsitta* because of the amount of missing data in this clade was high. We estimated subclade trees in IQ-TREE following the same procedures described above to produce alternative topologies (T_1 and T_2) estimated from alignments with (T_1) and without missing data (T_2). Each tree was rooted with a single outgroup (*Oreopsittacus arfaki* for *Charmosyna*, *Vini*, and *Phigys*; *P. goldiei* for all other clades) using phyx (Brown et al. 2017). We performed the same site-specific log-likelihood procedure described above for two alternative topologies (T_1 and T_2) except that site-likelihoods were converted to gene-wise log-likelihoods to assess the impact of missing data across an entire locus by summing the site-likelihoods for each gene using the scripts in Walker et al. (2018). We then estimated the Δ gene-wise log-likelihoods (hereafter Δ g-lk).

To explore how these putatively biased loci impacted phylogenetic inference, we grouped loci into bins representing Δ g-lk scores of: > 2, > 10, > 20, < -2, and < -10 (there were no genes where Δ g-lk

< -20 in the Filtered dataset). We followed the same procedure for producing concatenated alignments corresponding to each likelihood threshold bin, but for this step we excluded the outlier loci from the global concatenated alignment. We then estimated phylogenies from each alignment to assess how sensitive phylogenetic relationships were to excluding loci in each of these approaches. If missing data biases phylogenetic relationships then the exclusion of loci with positive Δ g-lk should alter relationships driven by missing data. The removal of loci with negative Δ g-lk will enhance relationships driven by biases in missing data.

Summarizing phylogenetic signal in modern and historical samples

To explicitly compare the information content in DNA sequence from historical and modern samples, we calculated alignment statistics for each locus and for alignments of only parsimony informative sites partitioned into sample types using AMAS (Borowiec 2016). We compared the amount of parsimony informative sites and missing data in samples with their age. Because we sequenced samples over multiple years, batch effects, or biases attributable to differences among sequencing run could also bias our results (Leigh et al. 2018). To provide a qualitative assessment of batch effects, we provide plots of trees where tips have been colored according to one of three plates that they were sequenced on. If there were substantial batch effects in the data then phylogenetic relationships could be, in part, due to whether samples were sequenced together.

We built a neural net in the R package caret v. 6.0.79 (Kuhn 2008) to test whether the Δ gene-wise log-likelihood of each gene partition could be predicted by the alignment statistics. The alignment statistics (alignment length, number of undetermined characters, the number of parsimony informative sites, number of variable sites, and GC content) were specified as the input neurons, and the output neuron was the Δ log-likelihood. The input data were scaled to the min and max for each statistic, and the percentage of training/test data was set to 75%/25%, respectively. We produced a 100 training/test datasets, independently ran each analysis, and report mean R^2, RSME, and variable importance. We performed this analysis on the Low Coverage alignment that included all taxa and independently on the six sub-clades using the data from both filtering schemes.

References

Amadon D. 1943. Birds collected during the Whitney South Sea Expedition. LII, Notes on some non-passerine genera, 3. Am. Mus. Novit. 1237:1–22.

Andersen MJ, Fatdal L, Mauck III WM, Smith BT. 2017. An ornithological survey of Vanuatu on the islands of Éfaté, Malakula, Gaua, and Vanua Lava. Check List 13:755–782.

Andersen MJ, McCullough JM, Mauck WM III, Smith BT, Moyle RG. 2018. A phylogeny of kingfishers reveals an Indomalayan origin and elevated rates of diversification on oceanic islands. J. Biogeogr. 45:269–281.

Andersen MJ, McCullough JM, Friedman NR, Peterson AT, Moyle RG, Joseph L, Nyári ÁS. 2019. Ultraconserved elements resolve genus-level relationships in a major Australasian bird radiation (Aves: Meliphagidae). Emu – Austral Ornithology 119:218–232.

Arcila D, Ortí G, Vari R, Armbruster JW, Stiassny ML, Ko KD, Sabaj MH, Lundberg J, Revell LJ, Betancur-R R. 2017. Genome-wide interrogation advances resolution of recalcitrant groups in the tree of life. Nat. Ecol. Evol. 1:0020.

Bolger AM, Lohse M, Usadel B. 2014. Trimmomatic: A flexible trimmer for Illumina sequence data. Bioinformatics 30:2114–2120.

Borowiec ML. 2016. AMAS: a fast tool for alignment manipulation and computing of summary statistics. PeerJ 4:e1660.

Briggs AW, Stenzel U, Johnson PL, Green RE, Kelso J, Prüfer K, Meyer M, Krause J, Ronan MT, Lachmann M, et al. 2007. Patterns of damage in genomic DNA sequences from a Neandertal. Proc. Natl. Acad. Sci. U.S.A, 104:14616–14621.

Brown JM, Thomson RC. 2017. Bayes factors unmask highly variable information content, bias, and extreme influence in phylogenomic analyses. Syst. Biol. 66:517–530.

Brown JW, Walker JF, Smith SA. 2017. Phyx: phylogenetic tools for unix. *Bioinformatics*, *33*(12):1886–1888.

Chakrabarty P, Faircloth, BC, Alda, F, Ludt, WB, McMahan, CD, Near, TJ, Dornburg, A, Albert, JS, Arroyave, J, Stiassny, M.L, et al. 2017. Phylogenomic systematics of ostariophysan fishes: Ultraconserved elements support the surprising non-monophyly of characiformes. Syst. Biol. 66(6):881–895.

Chernomor O, von Haeseler A, Minh BQ. 2016. Terrace aware data structure for phylogenomic inference from supermatrices. Syst. Biol. *65*(6):997–1008.

Clements JF, Schulenberg TS, Iliff MJ, Billerman SM, Fredericks TA, Sullivan BL, Wood CL. 2019. The eBird/Clements Checklist of Birds of the World: v2019. Downloaded from https://www.birds.cornell.edu/clementschecklist/download/

Dickinson EC, Remsen Jr JV. 2013. The Howard and Moore complete checklist of the birds of the world, Volume 1: Non-passerines. Edition: 4.

Enk JM, Devault AM, Kuch M, Murgha YE, Rouillard JM, Poinar HN. 2014. Ancient whole genome enrichment using baits built from modern DNA. Mol. Biol. Evol. 31:1292–1294.

Esselstyn JA, Oliveros CH, Swanson MT, Faircloth BC. 2017. Investigating difficult nodes in the placental mammal tree with expanded taxon sampling and thousands of ultraconserved elements. Genome Biol. Evol. 9:2308–2321.

Ewart KM, Johnson RN, Ogden R, Joseph L, Frankham GJ, Lo N. 2019. Museum specimens provide reliable SNP data for population genomic analysis of a widely distributed but threatened cockatoo species. Mol. Ecol. Resour. https://doi.org/10.1111/1755-0998.13082.

Faircloth BC, McCormack JE, Crawford NG, Harvey MG, Brumfield RT, Glenn TC. 2012. Ultraconserved elements anchor thousands of genetic markers spanning multiple evolutionary timescales. Syst. Biol. 61:717–726.

Faircloth BC. 2013. illumiprocessor: a trimmomatic wrapper for parallel adapter and quality trimming. http://dx.doi.org/10.6079/J9ILL.

Faircloth BC. 2015. PHYLUCE is a software package for the analysis of conserved genomic loci. Bioinformatics *32*:786–788.

Faircloth BC, Branstetter MG, White ND, Brady SG. 2015. Target enrichment of ultraconserved elements from arthropods provides a genomic perspective on relationships among Hymenoptera. Mol. Ecol. Resour. 15:489–501.

Forshaw JM. 2010. Parrots of the world. Wiltshire, UK: D & N Publishing.

Forshaw JM, Cooper WT. 1989. Parrots of the world. London: Blandford.

Fortes GG, Grandal‑d'Anglade A, Kolbe B, Fernandes D, Meleg IN, García‑Vázquez A, Pinto‑Llona AC, Constantin S, de Torres TJ, Ortiz JE, Frischauf C. 2016. Ancient DNA reveals differences in behaviour and sociality between brown bears and extinct cave bears. Mol. Ecol. 25:4907-4918.

Gilbert PS, Wu J, Simon MW, Sinsheimer JS, Alfaro ME. 2018. Filtering nucleotide sites by phylogenetic signal to noise ratio increases confidence in the Neoaves phylogeny generated from ultraconserved elements. Mol. Phylogenet. Evol. 126:116–128.

Gill F, Donsker D. 2019. IOC world bird list v9.2. DOI:10.14344/IOC.ML.9.2.

Grabherr MG, Haas BJ, Yassour M, Levin JZ, Thompson DA, Amit I, Adiconis X, Fan L, Raychowdhury R, Zeng Q, et al. 2011. Trinity: reconstructing a full-length transcriptome without a genome from RNA-Seq data. Nature Biotechnology 29(7):644.

Harvey MG, Smith BT, Glenn TC, Faircloth BC, Brumfield RT. 2016. Sequence capture versus restriction site associated DNA sequencing for shallow systematics. Syst. Biol. 65: 910–924.

Helgen KM, Pinto CM, Kays R, Helgen LE, Tsuchiya MT, Quinn A, Wilson DE, Maldonado JE. 2013. Taxonomic revision of the olingos (Bassaricyon), with description of a new species, the Olinguito. ZooKeys 324:1–83.

Hovmöller R, Knowles LL, Kubatko LS. 2013. Effects of missing data on species tree estimation under the coalescent. Mol. Phylogenet. Evol. 69(3):1057–1062.

Hosner PA, Faircloth BC, Glenn TC, Braun EL, Kimball RT. 2016. Avoiding missing data biases in phylogenomic inference: an empirical study in the landfowl (Aves: Galliformes). Mol. Biol. Evol. 33:1110–1125.

Huang H, Knowles LL. 2014. Unforeseen consequences of excluding missing data from next-generation sequences: simulation study of RAD sequences. Syst. Biol. 65:357–365.

Hung CM, Shaner PJL, Zink RM, Liu WC, Chu TC, Huang WS, Li SH. 2014. Drastic population fluctuations explain the rapid extinction of the passenger pigeon. Proc. Natl. Acad. Sci. U.S.A. 111:10636–10641.

Kehlmaier C, Barlow A, Hastings AK, Vamberger M, Paijmans JL, Steadman, D.W., Albury, NA, Franz R, Hofreiter M, Fritz U. 2017. Tropical ancient DNA reveals relationships of the extinct Bahamian giant tortoise *Chelonoidis alburyorum*. Proc. R. Soc. B. 284:20162235.

Jiang W, Chen SY, Wang H, Li DZ, Wiens JJ. 2014. Should genes with missing data be excluded from phylogenetic analyses? Mol. Phylogenet. Evol. 80:308–318.

Joseph L, Toon A, Schirtzinger EE, Wright TF, Schodde R. 2012. A revised nomenclature and classification for family-group taxa of parrots (Psittaciformes). Zootaxa 3205(2):26-40.

Kalyaanamoorthy S, Minh BQ, Wong TK, von Haeseler A, Jermiin LS. 2017. ModelFinder: fast model selection for accurate phylogenetic estimates. Nature Methods 14(6):587.

Katoh K, Standley DM. 2013. MAFFT multiple sequence alignment software version 7: improvements in performance and usability. Mol. Biol. Evol. 30(4):772–780.

Kratter AW, Kirchman JJ, Steadman DW. 2006. Upland bird communities on Santo, Vanuatu, Southwest Pacific. Wilson J. Ornithol. 118: 295–308.

Kück P, Longo GC. 2014. FASconCAT-G: extensive functions for multiple sequence alignment preparations concerning phylogenetic studies. Frontiers in Zoology, 11(1):81.

Kuhn M. 2008. Caret package. J. Stat. Softw. 28:1–26.

Leigh DM, Lischer HEL, Grossen C, Keller LF. 2018. Batch effects in a multiyear sequencing study: False biological trends due to changes in read lengths. Mol. Ecol. Resour. 18(4):778–788.

Lemmon AR, Brown JM, Stanger-Hall K, Lemmon EM. 2009. The effect of ambiguous data on phylogenetic estimates obtained by maximum likelihood and Bayesian inference. Syst. Biol. 58:130–145.

Li H, Durbin R. 2009. Fast and accurate short read alignment with Burrows-Wheeler transform. Bioinformatics. 25:1754–60.

Li H, Handsaker B, Wysoker A, Fennell T, Ruan J, Homer N, Marth G, Abecasis G, Durbin R, 1000 Genome Project Data Processing Subgroup. 2009. The sequence alignment/map (SAM) format and SAMtools. Bioinformatics. 25:2078–2079.

Linck EB, Hanna ZR, Sellas A, Dumbacher JP. 2017. Evaluating hybridization capture with RAD probes as a tool for museum genomics with historical bird specimens. Ecol. Evol. 7:4755–4767 .

Malmström H, Storå J, Dalén L, Holmlund G, Götherström A. 2005. Extensive human DNA contamination in extracts from ancient dog bones and teeth. Mol. Biol. Evol. 22:2040–2047.

Mayr E. 1933. Birds collected during the Whitney South Sea Expedition. 24, Notes on Polynesian flycatchers and a revision of the genus *Clytorhynchus* Elliot. Am. Mus. Novit. 628:1–21.

Mayr E. 1938. Birds collected during the Whitney South Seas Expedition, XL. Am. Mus. Novit. 522:1–22.

Mayr E. 1942. Birds collected during the Whitney South Sea Expedition. 48, Notes on the Polynesian species of *Aplonis*. Am. Mus. Novit. 1166:1–8.

McCormack JE, Hird SM, Zellmer AJ, Carstens BC, Brumfield RT. 2013. Applications of next-generation sequencing to phylogeography and phylogenetics. Mol. Phylogenet. Evol. 66:526–538.

McCormack JE, Tsai WL, Faircloth BC. 2016. Sequence capture of ultraconserved elements from bird museum specimens. Mol. Ecol. Resour. 16:1189-1203.

McCullough JM, Moyle RG, Smith BT, Andersen MJ. 2019. A Laurasian origin for a pantropical bird radiation is supported by genomic and fossil data (Aves: Coraciiformes). Proc. R. Soc. B 286(1910):20190122.

Mclean BS, Bell KC, Allen JM, Helgen KM, Cook JA. 2018. Impacts of inference method and data set filtering on phylogenomic resolution in a rapid radiation of ground squirrels (Xerinae: Marmotini). Syst. Biol. 68(2):298-316.

Merwin JT, Seeholzer GF, Smith BT. 2019. Macroevolutionary bursts and constraints generate a rainbow in a clade of tropical birds. bioRxiv 489419.

Mitchell KJ, Llamas B, Soubrier J, Rawlence NJ, Worthy TH, Wood J, Lee MS, Cooper A. 2014. Ancient DNA reveals elephant birds and kiwi are sister taxa and clarifies ratite bird evolution. Science 344:898–900.

Mitchell KJ, Scanferla A, Soibelzon E, Bonini R, Ochoa J, Cooper, A. 2016. Ancient DNA from the extinct South American giant glyptodont *Doedicurus* sp. (Xenarthra: Glyptodontidae) reveals that glyptodonts evolved from Eocene armadillos. Mol. Ecol. 25:3499–3508.

Mivart ST G. 1896. A monograph of the lories, or brush-tongued parrots, composing the family Loriidae. London: R.H. Porter.

Molloy EK, Warnow, T. 2017. To include or not to include: the impact of gene filtering on species tree estimation methods. Syst. Biol. 67:285–303.

Moyle RG, Oliveros CH, Andersen MJ, Hosner PA, Benz BW, Manthey JD, Travers SL, Brown RM, Faircloth BC. 2016. Tectonic collision and uplift of Wallacea triggered the global songbird radiation. Nat. Commun. 7:12709.

Nguyen LT, Schmidt HA, von Haeseler A, Minh BQ. 2014. IQ-TREE: a fast and effective stochastic algorithm for estimating maximum-likelihood phylogenies. Mol. Biol. Evol. 32:268–274.

Paijmans JL, Barnett R, Gilbert MTP, Zepeda-Mendoza ML, Reumer JW, de Vos J, Zazula G, Nagel D, Baryshnikov GF, Leonard JA, et al. 2017. Evolutionary history of saber-toothed cats based on ancient mitogenomics. Cur. Biol. 27: 3330–3336.

Paradis E, Claude J, Strimmer K. 2004. APE: analyses of phylogenetics and evolution in R language. Bioinformatics 20:289–290.

Philippe H, Snell EA, Bapteste E, Lopez P, Holland PW, Casane D. 2004. Phylogenomics of eukaryotes: impact of missing data on large alignments. Mol. Biol. Evol. 21:1740–1752.

Provost KL, Joseph L, Smith BT. 2018. Resolving a phylogenetic hypothesis for parrots: implications from systematics to conservation. Emu – Austral Ornithology 118:7–21.

R Core Team. 2019. R: A language and environment for statistical computing. R Foundation for Statistical Computing, Vienna, Austria. URL http://www.R-project.org/.

Revell LJ. 2012. phytools: an R package for phylogenetic comparative biology (and other things). Methods Ecol. Evol. 3:217–223.

Robinson DF, Foulds LR. 1981. Comparison of phylogenetic trees. Math. Biosci. 53:131–147.

Roure B, Baurain D, Philippe H. 2012. Impact of missing data on phylogenies inferred from empirical phylogenomic data sets. Mol. Biol. Evol. 30:197–214.

Ruane S, Austin CC. 2017. Phylogenomics using formalin‑fixed and 100+ year‑old intractable natural history specimens. Mol. Ecol. Resour. 17:1003–1008.

Sawyer S, Krause J, Guschanski K, Savolainen V, Pääbo S. 2012. Temporal patterns of nucleotide misincorporations and DNA fragmentation in ancient DNA. PloS ONE 7:e34131.

Schweizer M, Wright TF, Peñalba JV, Schirtzinger EE, Joseph L. 2015. Molecular phylogenetics suggests a New Guinean origin and frequent episodes of founder-event speciation in the nectarivorous lories and lorikeets (Aves: Psittaciformes). Mol. Phylogenet. Evol. 90:34–48.

Shavit Grievink L, Penny D, Holland BR. 2013. Missing data and influential sites: choice of sites for phylogenetic analysis can be as important as taxon sampling and model choice. Genome Biol. Evol. 5:681–687.

Shen XX, Hittinger CT, Rokas A. 2017. Contentious relationships in phylogenomic studies can be driven by a handful of genes. Nat. Ecol. Evol. 1:126.

Simmons MP. 2012. Radical instability and spurious branch support by likelihood when applied to matrices with non-random distributions of missing data. Mol. Phylogenet. Evol. 62:472–484.

Simmons MP. 2014. A confounding effect of missing data on character conflict in maximum likelihood and Bayesian MCMC phylogenetic analyses. Mol. Phylogenet. Evol. 80:267–280.

Smith BT, Harvey MG, Faircloth BC, Glenn TC, Brumfield RT. 2014. Target capture and massively parallel sequencing of ultraconserved elements for comparative studies at shallow evolutionary time scales. Syst. Biol. 63(1):83–95.

Springer MS, Gatesy J. 2018. On the importance of homology in the age of phylogenomics. Syst. Biodivers. 16:210–228.

Stamatakis A. 2014. RAxML version 8: a tool for phylogenetic analysis and post-analysis of large phylogenies. Bioinformatics. 30:1312–1313.

Streicher JW, Schulte JA, Wiens JJ. 2015. How should genes and taxa be sampled for phylogenomic analyses with missing data? An empirical study in iguanian lizards. Syst. Biol. 65:128–145.

Thomas RH, Schaffner W, Wilson AC, Pääbo S. 1989. DNA phylogeny of the extinct marsupial wolf. Nature. 340:465.

Thom G, Amaral FRD, Hickerson MJ, Aleixo A, Araujo-Silva LE, Ribas CC, Choueri E, Miyaki CY. 2018. Phenotypic and genetic structure support gene flow generating gene tree discordances in an Amazonian floodplain endemic species. Syst. Biol. 67(4):700-718.

Tin MMY, Rheindt FE, Cros E, Mikheyev AS. 2015. Degenerate adaptor sequences for detecting PCR duplicates in reduced representation sequencing data improve genotype calling accuracy. Mol. Ecol. Resour. 15:329–336.

Walker JF, Brown JW, Smith SA. 2018. Analyzing contentious relationships and outlier genes in phylogenomics. Syst. Biol. 67(5):916–924.

Wiens JJ, Morrill MC. 2011. Missing data in phylogenetic analysis: reconciling results from simulations and empirical data. Syst. Biol. 60:719–731.

Wingett SW, Andrews S. 2018. FastQ Screen: A tool for multi-genome mapping and quality control. F1000Research 7.

Xi Z, Liu L, Davis CC. 2015. The impact of missing data on species tree estimation. Mol. Biol. Evol. 33:838-860.

Yao L, Li H, Martin RD, Moreau CS, Malhi RS. 2017. Tracing the phylogeographic history of Southeast Asian long-tailed macaques through mitogenomes of museum specimens. Mol. Phylogenet. Evol. 116:227–238.

SUPPLEMENTARY TABLE LEGENDS

Supplementary Table 1. Metadata for Loriini samples used in this study.

Supplementary Table 2. Neural Net model output for subclades that assessed predictors of Δ gene-wise log-likelihood scores Shown are the variable importance of the five alignment statistics included in the neural net model for each subclade in Loriini. a) *Eos*, *Trichoglossus*, *Glossopsitta concinna*, and *Psitteuteles iris*, b) *Parvipsitta* and *Psitteuteles*, c) *Neospittacus*, d) *Chalcopsitta* and *Pseudeos*, e) *Lorius*, and f) *Charmosyna*, *Vini*, and *Phigys*. The per locus statistics were as follows: parsimony informative sites (PIS), alignment length (Ali. Len.), number of variables sites (Var. Sites), number of undetermined characters (Undet. Char.), and GC content (GC. content). The sample size for each subclade was the total number of alignments and 75%/25% was used to train/test each model. Reported are R^2 and mean square error (MSE).

SUPPLEMENTARY FIGURE LEGENDS

Supplementary Figure S1. Sampling map of lory and lorikeet taxa used in this study. Colored symbols represent material that came from historical (blue) and modern (red) samples.

Supplementary Figure S2. Likelihood plots showing gene Δ gene-wise log-likelihoods for topologies estimated with and without missing data for the Filtered dataset. The y-axis is the Δ gene-wise log-likelihood and the x-axis represents individual loci across the full alignment. Shown are the results for six subclades assessed within Loriini using the Filtered dataset: A) *Parvipsitta* and *Psitteuteles*, B) *Chalcopsitta* and *Pseudeos*, C) *Neospittacus*, D) *Charmosyna*, E) *Eos*, *Trichoglossus*, and *Psitteuteles*

iris, and F) *Lorius*. Points are colored according to the magnitude of the Δ gene-wise log-likelihood scores using a gradient ranging from > 20 (blue) through < -10 (orange).

Supplementary Figure S3–S8. Low Coverage maximum likelihood trees. The tree was inferred from a concatenated alignment with all loci (fig. S3) and an increasing number of loci excluded in increments of the Δ gene-wise log-likelihood scores of: (Δ s-lk) thresholds of: >20 (fig. S4), >10 (fig. S5), >2 (fig. S6), <-10 (fig. S7), and <-2 (fig. S8). On each node are shown bootstrap values. Tip labels are colored according to whether the sample came from a historical (blue) or modern (red) sample.

Supplementary Figure S9–S14. Filtered maximum likelihood trees. The tree was inferred from a concatenated alignment with all loci (fig. S9) and an increasing number of loci excluded in increments of the Δ gene-wise log-likelihood scores of: (Δ s–lk) thresholds of: >20 (fig. S10), >10 (fig. S11), >2 (fig. S12), <-10 (fig. S13), and <-2 (fig. S14). Bootstrap values are shown on each node. Tip labels are colored according to whether the sample came from a historical (blue) or modern (red) sample.

Supplementary Figure S15. Plot showing that older samples have more missing data. Shown is the year the sample was collected at the percentage of missing characters as determined by IQ-TREE. Mean regression line and 95% CI are shown (Adjusted R^2 = 0.51; n = 144; p-value < 0.0001). Not all samples were included in this analysis because accurate ages of the specimens were unavailable.

Supplementary Figure S16 and S17. Low Coverage and Filtered maximum likelihood trees with all samples (*N* = 171) and tips colored by sequencing plate. Presented are Low Coverage (fig. S16) and Filtered (fig. S17) trees where tips were colored according to one of three (Plate 1: red; Plate 2: orange; and Plate 3: blue) lanes, which were sequenced independently over the course of three years.

Supplementary Figure S18 and S19. Low Coverage and Filtered maximum likelihood trees with all samples (*N* = 171) and tips colored according to sample type. Presented are Low Coverage (fig. S18) and Filtered (fig. S19) trees where tips are colored according to whether the sample type came from a historical specimen (blue) or modern tissue (red).

29